Effects induced by Mie resonance in two-dimensional photonic crystals



2007 J. Phys.: Condens. Matter 19 176214

(http://iopscience.iop.org/0953-8984/19/17/176214)

IOP PUBLISHING JOURNAL OF PHYSICS: CONDENSED MATTER

J. Phys.: Condens. Matter **19** (2007) 176214 (12pp) doi:10.1088/0953-8984/19/17/176214

# Effects induced by Mie resonance in two-dimensional photonic crystals

**Lina Shi**[1,2], **Xunya Jiang**[1] **and Chengfang Li**[2]

[1] National Key-Laboratory of the Functional Material, Shanghai Institute of Microsystem and Information Technology, CAS, Shanghai 200050, People's Republic of China
[2] Department of Physics, Wuhan University, Wuhan 430072, People's Republic of China

E-mail: xyjiang@mail.sim.ac.cn

Received 27 November 2006, in final form 8 March 2007
Published 30 March 2007
Online at stacks.iop.org/JPhysCM/19/176214

**Abstract**

The effects of Mie resonance on the photonic band-gap structure of two-dimensional photonic crystals are investigated in detail. Firstly, we demonstrate the correlation between the band-gap structure and Mie resonance, such as the midgap frequency and the changes in gap width with different cylinder radii. We find that the midgap frequency and the gap width increase linearly and then saturate, before and after the Mie resonance frequency crosses the midgap frequency. The radius value at the crossing point between the midgap frequency and the Mie resonance frequency becomes smaller with the increase in the refractive contrast. For large radius, all the Mie resonance frequencies fall into the corresponding bands. Secondly, the changes in the gap width are studied with increasing index of the cylinders. Changing rules of the gap width are found depending on the position of the Mie resonance frequency. For example, when the Mie resonance falls inside the gap the gap width increases most rapidly and reaches its maximum value when the Mie resonance is leaving the gap range (around the lower edge of the gap). After that the gap width decreases very steeply with increase in the refractive contrast. Thirdly, we investigate the effect of Mie resonance on the band width for the 'heavy-photon band', which is the third band of our system. We find that, quite different from other bands, the band widths of such bands are determined by the overlapping integral of the Mie resonance states. All these results can be explained by the Mie resonance based on two physical pictures, i.e. the scattering picture and the hopping picture. According to these analyses and results, we may understand more clearly how the Mie resonances influence the formation of the band-gap structure. The Mie resonance effects on photonic band-gap structure presented in this paper would be valuable in designing various kinds of photonic crystals.

(Some figures in this article are in colour only in the electronic version)

  

## 1. Introduction

Photonic crystals (PCs) have attracted much attention recently since their rich dispersion relations enable one to control light with amazing facility and produce effects which are impossible with conventional optics. In order to fully utilize these dispersion properties of PCs we need to understand the origin of the photonic band-gap (PBG) structure. It is well known that besides the Bragg multiple scattering, there is also a second mechanism called Mie resonance [1, 2], that contributes to the formation of the spectral gaps. Mie resonance is the scattering excitation of a single scatterer. For higher dielectric contrast, it was suggested that Mie resonances of an isolated scatterer correspond to pseudogaps or flat bands in the band structure [3–5] and in PCs they play the same role as the atomic orbitals in the electronic case [6–8].

The discussion of effects induced by Mie resonances in PCs was initiated by John [9]. In a very early study, of three-dimensional system (e.g. an fcc lattice) John supposed 'a large photonic band gap arises when the density of dielectric spheres is chosen such that the Mie scattering resonance occurs at the same wavelength as the macroscopic Bragg resonance of the array'. Based on this idea, he found the optimum volume filling fraction $f = 1/(2n)$ (where $n$ is the refractive index) for the one-dimensional case. And Datta [10] concluded that for the scalar case there was indeed a strong correlation between the resonance frequencies of a single scatterer and the frequencies at which gaps appear. However, there are some differing opinions about the Mie resonance effect on the widening of the gap [11]. So the relation between the Mie resonance and the band-gap structure still needs more detailed investigation.

In this paper we make further investigation of effects induced by Mie resonance in PCs. We choose the 2D case and confine our attention to the TM mode. The advantage of a 2D system is that TM and TE modes are separate, which simplifies the nature of the eigenmodes and corresponding computation and makes it easier to understand the physical origin of the band-gap structure. Moreover, 2D PCs are more easily fabricated than 3D ones, so the study of the 2D case is meaningful for applications. Finally, the 2D case should be more interesting, since the 2D scattering effect is stronger than 3D but weaker than 1D. And the detailed quantitative investigation of effects induced by Mie resonance in PCs for the 2D case are left open from previous studies [9–11]. In this paper we examine the effects induced by Mie resonance on the band-gap structure of 2D PCs and give further qualitative and quantitative study of the correlation between Mie resonance and the formation of the photonic band gap. We find that with increasing radii the Mie resonance frequency and gap width increase almost linearly, then the midgap frequency crosses the Mie resonance frequency, finally becoming saturated. For a large radius, the Mie resonance frequency falls in the band. The gap can be enlarged when Mie resonance falls near the low edge of a gap. The width of the third band dominated by Mie resonance corresponds to the overlapping integral. We explain these behaviours from the field distribution in PCs.

This paper is constructed as follows. In section 2 we compare Mie resonance frequencies of a single cylinder with the band-gap structure to look for any correlation between them. The effect of Mie resonance on the gap width is the subject of section 3. Section 4 is devoted to the effect of Mie resonance on the band width. A conclusion is finally drawn in section 5. In addition, the selection of the second gap is discussed in the appendix.

## 2. The correlation between Mie resonances and gaps

In this section, we will compare the 2D band-gap structure with the Mie resonance frequencies of a single cylinder to find the correlation between them. There are two well-known physical

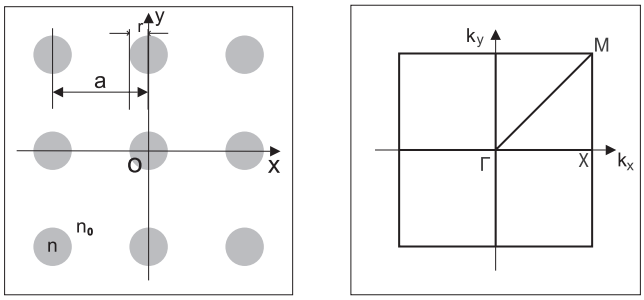


(a) cross section (b) the first Brillouin zone

**Figure 1.** (a) Cross section of 2D periodic dielectric cylinders of radius $r$ and lattice constant $a$, $r/a = 0.2$. The refractive index of the cylinders is $n$. The origin of coordinates is chosen at the centre of one of the cylinders. (b) The first Brillouin zone (BZ) of the square 2D PC. Γ, X and M is the high-symmetry points in the first BZ.

pictures of the effects of Mie resonance on photonic band-gap structures. The first one is the 'scattering picture' in which the back-scattering of a single scatterer (through Mie resonance) is important for the generation of a photonic gap. In this picture the Mie resonances act as an obstacle to the propagation of light in PCs. The second picture is the 'hopping picture' in which the photons can hop from one cylinder to another with the overlap of the Mie resonant states. In this picture, the Mie resonance can help the wave to propagate through the PC. So for a band-gap structure in a certain frequency range, the main effect of Mie resonance should be discussed more carefully.

We adopt the structure shown in figure 1(a). Infinitely long dielectric cylinders are arranged in a vacuum to form a square lattice in the $xy$ plane. The radius of cylinders and the lattice constant are denoted by $r$ and $a$, respectively. The refractive index of cylinders is denoted by $n$ and that one of the vacuum is $n_0 = 1$. The first Brillouin zone is plotted in figure 1(b). Only the E-polarized states and the several lower bands in the ΓX direction are discussed. The band-gap structure is calculated by the plane-wave method. We compare the first two Mie resonance frequencies and the low band-gap structure to look for the correlation between them. Our definition of 'the second gap' is quite different from the common sense one, which is defined as the energy range between the second band and *fifth* band. For detailed arguments about the definition please see the appendix.

To find the general rules of the band-gap structure from the Mie resonance, we plot Mie resonance frequencies (black squares) and the midgap frequencies (red dots) versus the ratio $r/a$ for different refractive contrasts in figure 2. Figures 2(a)–(f) are respectively for $n = 1.1, 1.7, 2.6, 3.6, 4.5$ and 10. The frequency is presented in units of $\omega r/2\pi c$, where $\omega$ is the angular frequency. In this unit the Mie resonance frequencies are independent of $r$ (only depend on the refractive index $n$), then the Mie resonance frequencies versus the radius are straight lines as shown in figure 2.

From figures 2(b)–(e), in which the refractive indices are in the normal value and range from 1.7 to 4.5, we can find some universality. (i) When the first (second) midgap frequency has not crossed the first (second) Mie resonance frequency, the midgap frequency and the gap width increase almost linearly with the increase in the cylinder radius. When the first (second) midgap frequency has crossed the first (second) Mie resonance frequency the increase in the midgap frequency obviously becomes slow and finally saturated. (ii) The radius value at the cross point of the first (second) midgap frequency and the first (second) Mie resonance frequency becomes smaller when the refractive index $n$ becomes larger. (iii) When the radius

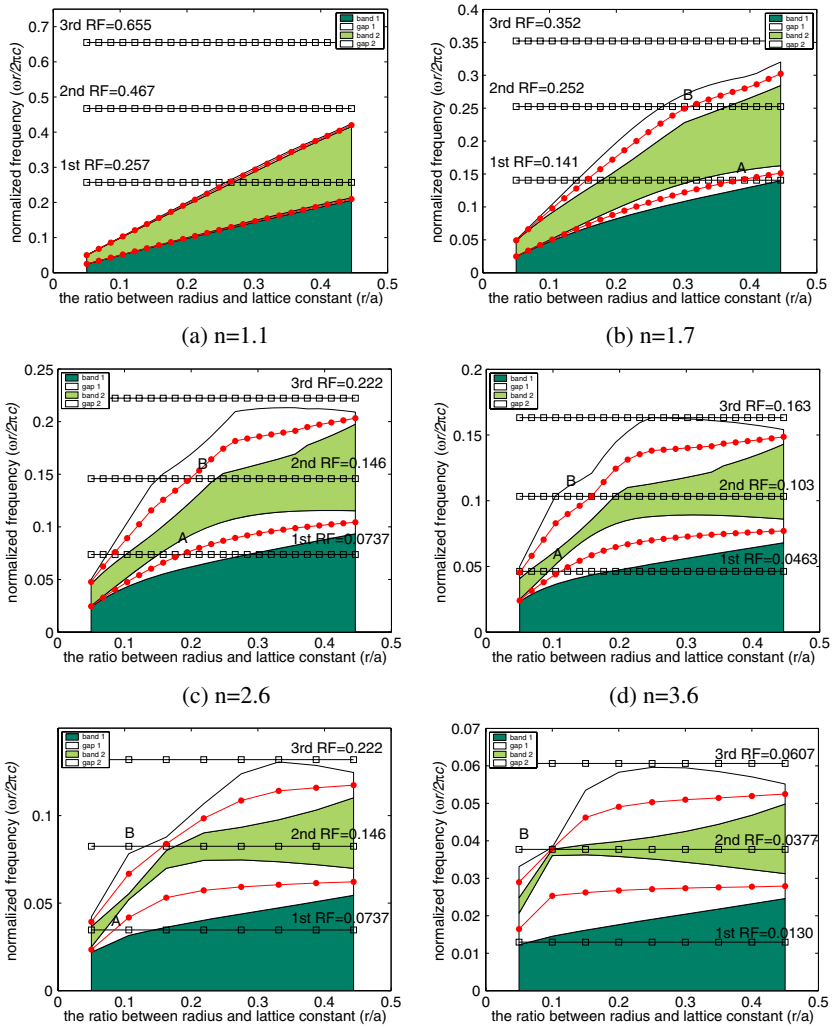


**Figure 2.** Mie resonance frequencies (black squares) and midgap frequencies (red dots) versus the ratio $r/a$. They cross at A and B. The frequency is presented as $\omega r/2\pi c$. (a) The refractive index $n = 1.1$, the first three Mie resonance frequencies and the first two midgap frequencies. (b) As (a) except $n = 1.7$. (c) As (a) except $n = 3.6$. (d) As (a) except $n = 3.6$. (e) As (a) except $n = 10$. (f) As (a) except $n = 10$.

of the cylinder is large ($>0.4$), for all refractive indices, the first (second) Mie resonance falls at the first (second) band. From these evident general behaviours we find that in the normal index range there is an apparent correlation between the Mie resonance and the band-gap structure.

We will give a qualitative explanation of the correlation between the Mie scattering and the band-gap structure from detailed analysis of the field propagation in the different conditions. The field distributions of Bloch waves can reveal some basic pictures for us especially for the midgap states. We note at here that the 'Bloch states' are generally defined at the band frequency range, but this concept can be broadened into the gap frequency range, when the modes are *evanescent* and the wavevector is complex [14]. In figures 3(a) and (b) by using the

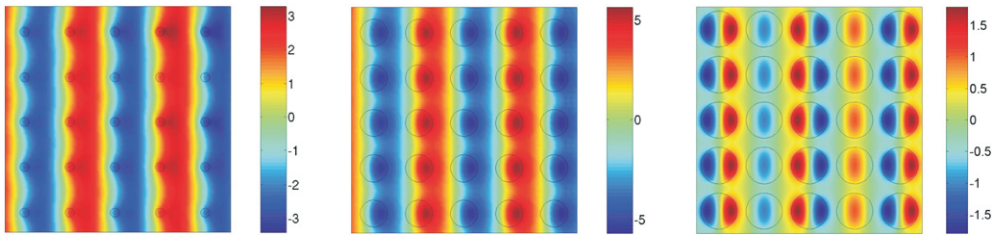


(a) r/a=0.1 (b) r/a=0.3 (c) r/a=0.4

**Figure 3.** (a) The field distributions of *the Bloch state of midgap frequency* with $\omega a/2\pi c = 0.4505$ for $r/a = 0.1$ ($n = 3$) simulated by FDTD. The exponential decay factor is cancelled. (b) As (a) except $\omega a/2\pi c = 0.2841$ for $r/a = 0.3$. (c) The field distribution of the mode at the second band for $k_x = 0.25$, $n = 3$ and $r/a = 0.4$ simulated by the plane wave method. The black circles denote the cylinders.

finite-domain time-dependent (FDTD) method we calculate the field distributions of *the Bloch state of midgap frequency* and plot them for $n = 3$ with $\omega a/2\pi c = 0.4505$ for $r/a = 0.1$ and $\omega a/2\pi c = 0.2841$ for $r/a = 0.3$, respectively. In the FDTD simulation, the plane wave with the midgap frequency from a line source is normally incident to the PC from the left. But since the frequency is inside the gap, the field should decay exponentially. In figures 3(a) and (b), the exponential decay factor is cancelled by hand to show the field distribution more clearly. For comparison, the field distribution of the Bloch state at the second band for $K_x = 0.25$ in a $n = 3$ and $r/a = 0.4$ system is obtained by the plane-wave method and plotted in figure 3(c). In these figures, the black circles denote the cylinders. In figure 3(a), the 'scattering picture' can be observed that the light is scattered off the propagation direction by cylinders. On the other hand, the 'hopping picture' is shown in figure 3(c) where the field is more concentrated in the dielectric region and the light can hop from one cylinder to another through the overlap of the Mie resonance states. In figure 3(b), we show the middle stage from the scattering picture to the hopping picture. We can see that the field is scattered similarly to figure 3(a). But the fields of different cylinders starts to overlap with each other, which is much more obvious in figure 3(c).

For the behaviour (i), when the radius is small, the field distribution shown in figure 3(a) is a typical example. From the field distribution of figure 3(a), the isolated cylinders scatter the propagating wave and so we adopt a scattering picture. In this case, the mechanism of the band-gap is dominated by the Bragg scattering effect, which is determined by the 'in phase' constructive interference of the back-scattered fractional waves from different scatters. Therefore, the gap position is mainly determined by the 'in phase' condition of back-scattered fractional waves, such as $2n_{\text{ave}}a\omega_{\text{gap-centre}}/c = 2\pi$, where $n_{\text{ave}} = \sqrt{f\epsilon + (1-f)\epsilon_0}$ ($\epsilon$ and $\epsilon_0$ are respectively the dielectric of the cylinder and the vacuum) is the average index in the PC and $f$ is the filling ratio. The normalized midgap frequency $f_{\text{gap-centre}} = \omega_{\text{gap-centre}}/(2\pi c/r) = (2\pi c/2n_{\text{ave}}a)r/2\pi c = r/2n_{\text{ave}}a$ is proportional to the radius of dielectric cylinder and $n_{\text{ave}} \simeq 1$ due to the small radius. This explains why the gap-centre frequency increases linearly with the increase of cylinder radius. However, the scattering strength (or cross-section) of individual cylinders is proportional to the radius of the cylinder, so that the gap width is proportional to the radius of the cylinders too. Now the Mie resonant frequency is a little distance from the gap central frequency, so that we cannot see the Mie resonance field distribution in figure 3(a). And since the Bragg condition is wavelength matching with the lattice spacing (a) while the Mie condition is wavelength matching with the cylinders of diameter ($2r$) and $2r < a$, the Bragg condition always falls below the first Mie resonance; thus the gap opens below the Mie

resonance. But when the radius of the cylinder is larger, the Mie resonance effect become more and more obvious. We find that the increase in midgap frequency can be saturated, especially after the gap-central frequency crosses the Mie resonant frequency (actually the gap width is also saturated, as will be discussed in section 3). This phenomenon can be explained by field distribution shown in figure 3(b). After the midgap frequency crosses the Mie resonance frequency, the field becomes more concentrated inside the cylinder. Then the effect of the increase in the radius becomes weaker in the change of the effective refractive index $n_{\text{eff}}$ (related with the field distribution), and therefore the midgap frequency becomes saturated. Here $n_{\text{eff}} = \sqrt{f_e * \epsilon + (1 - f_e) * \epsilon_0}$, where $f_e = \int_{V_\epsilon} E^*(r)D(r)\,\mathrm{d}^3r / \int E^*(r)D(r)\,\mathrm{d}^3r$ is related to the field distribution [13]. The filling ratio $f_e$ measures the fraction of electrical energy located inside the cylinders and is applicable to all bands.

For the behaviour (ii), when the radius is small the band-gap mechanism is dominated by the Bragg scattering effect and the midgap frequency ($f_{\text{gap-centre}} = \omega_{\text{gap-centre}} r/2\pi c$) increases linearly with the increase in cylinder radius for all refractive indices. Due to the small radius the scattering strength is weak and $n_{\text{eff}} \simeq 1$ for all refractive indices. But the normalized Mie resonance frequencies $f_{\text{Mr}} = \omega_{\text{Mr}} r/2\pi c$ decrease with the increase of the refractive index (in this unit it is independent of $r$). Then when the refractive index increases the lines denoting the midgap frequencies almost not change while the normalized Mie resonance frequencies $f_{\text{Mr}}$ go down. Therefore, the radius becomes smaller at the crossing point of the midgap frequency and the Mie resonance frequency. This is an important value for judging the saturation of the midgap frequency.

For the behaviour (iii), as the radius of the cylinder is very large ($r > 0.4a$) the field such as displayed in figure 3(c) is more concentrated in the dielectric region, and the propagation of waves is taking place by hopping from cylinder to cylinder through the overlap of the local resonance states. Now it is not surprising to find that the Mie resonance frequencies fall in bands for all dielectric constants. It is well-known that from the tight-binding model of atomic lattices the electronic band can be thought as the broadening of the single atomic states. This picture generally does not work for EM waves, since the Mie resonance is much weaker than the atomic bounded states. But the hopping picture which is widely used in the tight-binging model still can be used when the radius of the cylinders is large enough. This point agrees with Datta's [10] conclusion for the scalar case and is similar to the conclusion of the acoustic and elastic wave [15].

Now we discuss the two extreme cases. For the case of $n = 1.1$, the scattering of the single cylinder is so weak for all radii that the Bragg scattering dominates the band-gap structure. Therefore, in figure 2(a) the first (second) midgap frequency has not crossed the first (second) Mie resonance frequency and always increases with increasing radius. For the case of $n = 10$ in figure 2(f), the field concentrates its energy inside the cylinder more easily. So when the radius is small ($r/a = 0.1$) the first (second) midgap frequency crosses the first (second) Mie resonance frequency and falls into the first (second) band. The case of figure 2(f) is more like the tight-binding model of electronic systems [6].

## 3. The effects on the gap width by Mie resonance

In this section, different from previous discussion, we examine the correlation between the Mie resonance and the photonic gap width with fixed radius but changing refractive index.

With the refractive index increasing linearly, the first (second) gap width ($\Delta\omega/2\pi$) versus the normalized deviation of the Mie resonance from the gap centre ($(\omega_{\text{gc}} - \omega_{\text{Mr}})/\Delta\omega_g$) for the first and second gaps is plotted in figure 4. Between the two vertical lines there is the range where Mie resonance falls *inside* the gap. Figures 4(a)–(c) are the cases for the first gap with

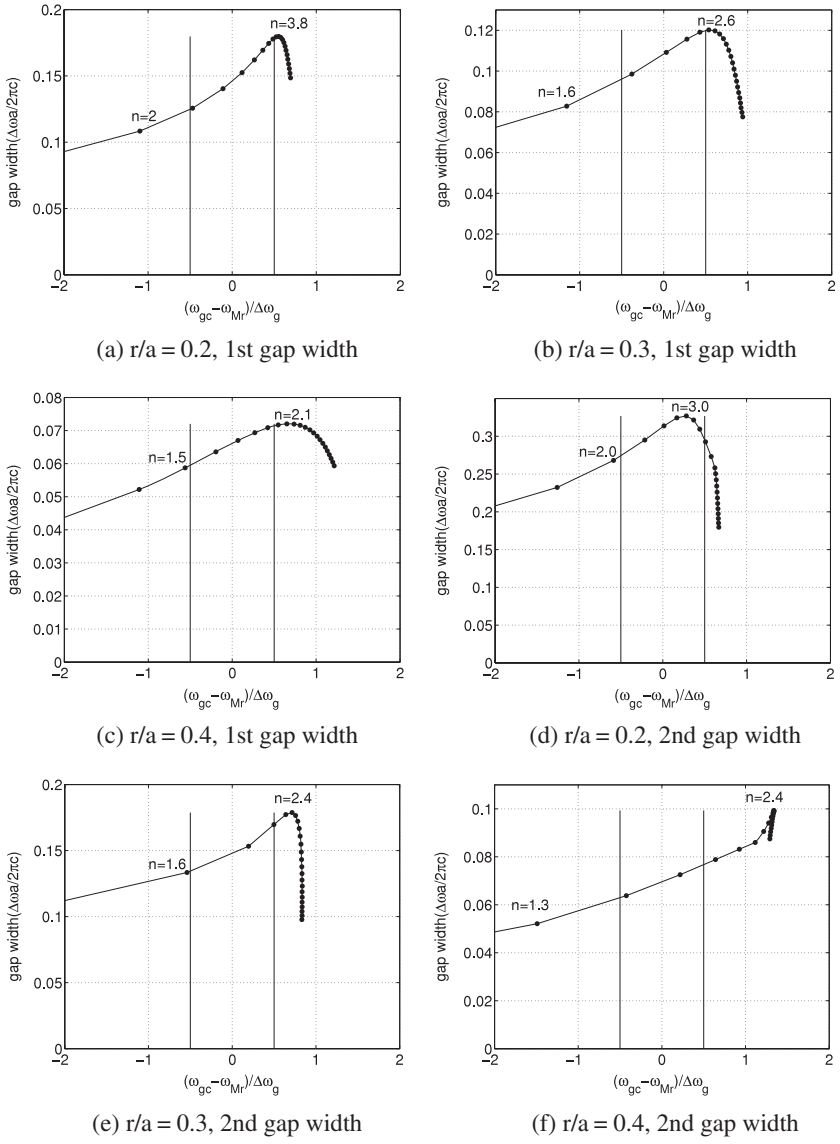


(a) r/a = 0.2, 1st gap width (b) r/a = 0.3, 1st gap width

(c) r/a = 0.4, 1st gap width (d) r/a = 0.2, 2nd gap width

(e) r/a = 0.3, 2nd gap width (f) r/a = 0.4, 2nd gap width

**Figure 4.** The gap width versus the place where the Mie resonance is located in the gap. A vertical line is plotted when Mie resonance falls at the edge of the gap. (a) The first gap for $r/a = 0.2$, (b) the first gap for $r/a = 0.3$, (c) the first gap for $r/a = 0.4$, (d) the second gap for $r/a = 0.2$, (e) the second gap for $r/a = 0.3$, (f) the second gap for $r/a = 0.4$.

$r/a = 0.2$, $r/a = 0.3$ and $r/a = 0.4$, respectively. And the other figures are the cases for the second gap with same radii.

From figure 4, it is evident that for a fixed radius, when the index is small, the Mie resonance frequency $\omega_{\mathrm{Mr}}$ is outside the gap (much larger than $\omega_{\mathrm{gc}}$) and the gap width is small. But with increasing index, $\omega_{\mathrm{Mr}}$ gradually moves into the gap range from the upper gap edge, and at the same time the gap width increases rapidly. When the Mie resonance frequency $\omega_{\mathrm{Mr}}$ gets into the gap, the gap width shows its most rapid increase in the whole process. But with

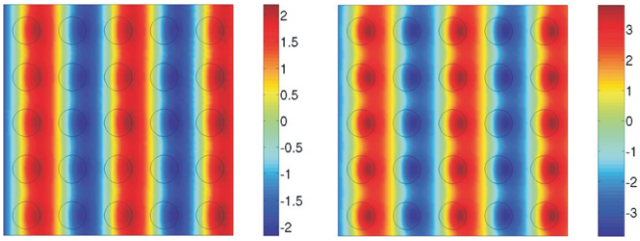


(a) $n = 1.6$ (b) $n = 2.6$

**Figure 5.** The field distributions of *the Bloch state of midgap frequency* with $\omega a/2\pi c = 0.435\,85$ for $n = 1.6$ and $r/a = 0.3$ by FDTD. The exponential decay factor is cancelled. (b) As (a) except $\omega a/2\pi c = 0.3123$ for $n = 2.6$.

the index becoming larger, around the range where the $\omega_{\mathrm{Mr}}$ pass the lower gap edge, we can find the gap width gets to its maximum value. After that the gap width decreases very steeply with increasing index.

We can understand the behaviours in figure 4 from the scattering effect of the Mie resonance plotted in figure 5. When the refractive index is low (the difference in index between the cylinder and vacuum is small), as we discussed before, the scattering picture still works. The band-gap structure is dominated by the Bragg scattering. With increasing refractive index the scattering cross-section becomes larger and the gap width increases rapidly. The phenomenon of the gap width increasing most quickly as the $\omega_{\mathrm{Mr}}$ gets into the gap from upper gap edge can be explained by the Mie resonance too. Obviously, in this case, the scattering effect of Mie resonance is strongest and mostly contributes to the photonic gap. Actually, this is exactly the condition that Sajeev John supposed where the Bragg scattering and the Mie resonance both mostly contribute to the gap generation. From the figures there is obviously a maximum gap width for a certain radius and the maximum value generally appears when the Mie resonance passes the lower gap edge. After the maximum gap-width point, the Mie resonance falls into the band frequency range and the gap width decreases sharply. This is reasonable since when the Mie resonance frequency falls into the band the scattering effect of Mie resonance should be much weaker and the hopping picture becomes dominating.

For our discussion, we can see that the gap width which is an important value for the design of the PC is closely related with the Mie resonance. This not only reveals the deep relation between the band-gap structure and the Mie resonance, but also helps us to optimize the design of the PC for a large gap.

## 4. The effects on the 'heavy-photon' band width by Mie resonance

As we have discussed, the hopping picture based on the Mie resonance can help us to understand the corresponding relation between the photonic band and Mie resonance. For the 2D photonic crystal which we have studied in previous sections there is a special band, the third band, which is called the 'heavy-photon' band [4, 5] in other studies. Under certain conditions, the third band of the 2D photonic structure shows an extraordinary property: the band width is very small. Or in other words, it is a very flat band which means that the group velocity of the band modes is very small (so that it is called the 'heavy-photon' band). We will see that this property is closely related to Mie resonance.

In this section we will discuss the effects of Mie resonance on the band width in detail. We plot the first three band widths versus the refractive index for different radii ($r = 0.2a$–$0.45a$) in

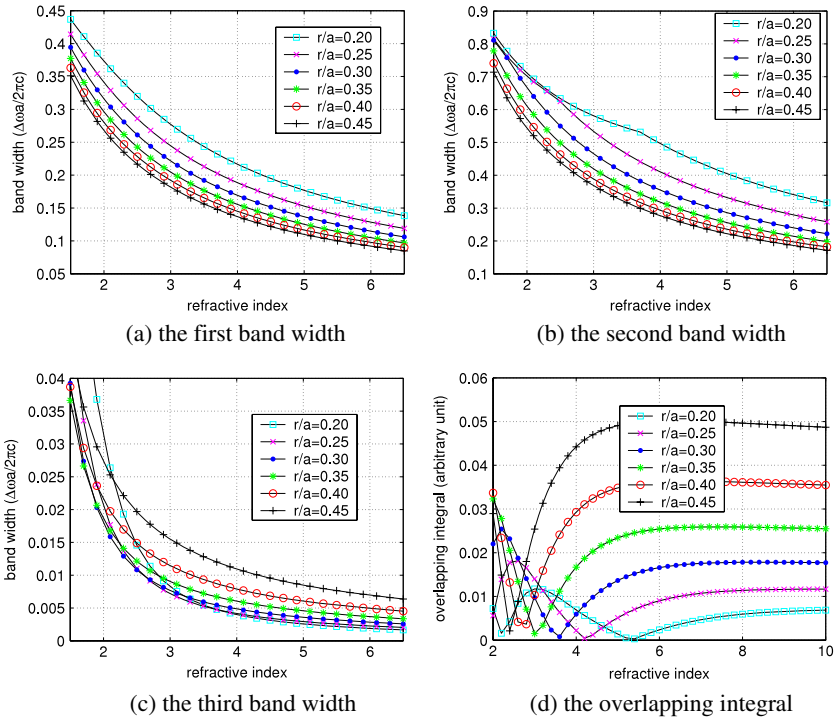


(a) the first band width (b) the second band width

(c) the third band width (d) the overlapping integral

**Figure 6.** (a) The first band widths ($\Delta\omega/2\pi$) versus the refractive index for different radius. (b) The second band width. (c) The third band width. (d) The overlapping integral (arbitrary unit) versus the refractive index for different radius.

figures 6(a)–(c) respectively. Figures 6(a)–(c) show that the band widths of all bands decrease with increasing refractive index. But more detailed observation of figure 6(c), which is of the third band, shows that it is quite different from the first band (figure 6(a)) and the second band (figure 6(b)). First the band width of the third band is about 1 to 2 orders smaller than other two bands, and this is why the third band is called the 'heavy-photon' band. Second the radius sequence of figure 6(c) is different from other two bands when the index is large enough ($n > 3$). In figure 6(c), the curves from top to bottom are in the sequence that the radius is decreasing, while in figures 6(a) and (b) the curves from top to bottom are in the sequence that the radius is increasing. In other words, the band width of the first and second bands decreases with increase in the radius, while the band width of the third band increases. In order to understand these behaviours we plot the field distributions of the modes at the first, second and third bands for $k_x = 0.25$, $n = 4$ and $r/a = 0.2$ in figure 7, respectively.

From the field distribution of the modes calculated by the plane-wave method in figure 7, first we can explain why the third band is very flat, which means the frequency of the band is almost independent of the $K_x$ (Bloch vector) variation. In figure 7 we can see that the Mie resonance 'direction' of the third band is in the $y$ direction, which is perpendicular to the wave propagation direction (the $x$ direction). If we write the frequency of the Bloch mode in a band approximately as $\omega^2 = (Q_x^2 + Q_y^2)c^2/\epsilon\mu$, where $Q_x$ and $Q_y$ are the local values of $\partial_x E(x, y)$ and $\partial_y E(x, y)$, respectively, where $E(x, y)$ is the field inside the photonic crystal. For the second band, $Q_y$ is zero, and $Q_x$ has two parts, one part from the Mie resonance $K_M$ and the other from the Bloch vector $K_x$. So the frequency of the second band can be shown as

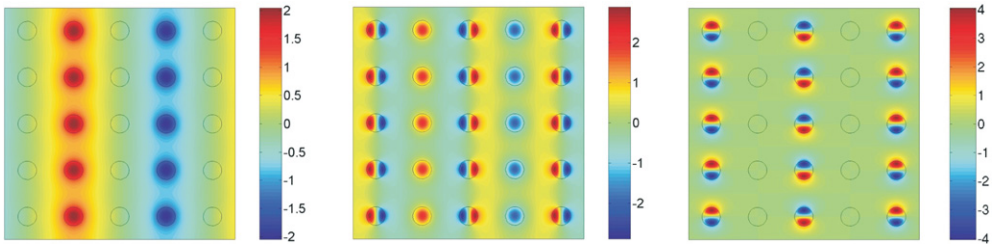


(a) 1st band (b) 2nd band (a) 3rd band

**Figure 7.** The field distribution of the mode at the first three bands for $k_x = 0.25$, $r/a = 0.2$ and $n = 4$. The black circles denote the cylinders. (a) For the first band. (b) For the second band. (c) For the third band.

$\omega^2 = (K_M + K_x)^2c^2/\epsilon\mu \approx (K_M^2 + 2K_M K_x)c^2/\epsilon\mu$ when $K_M >> K_x$. But for the third band, since the Mie resonance is in the $y$ direction, so that $Q_y = K_M$, and it is a large value compared with $Q_x = K_x$ which is in the range $(0, G/2)$. The frequency of the third band is $\omega^2 = (K_M^2 + K_x^2)c^2/\epsilon\mu$, which is obviously almost independent of the second-order small value $K_x^2$. From the field distribution, we can guess that the value of $Q_y$ is larger than $2G$. So the normalized band width $\Delta\omega_b/\omega_b$ (where $\Delta\omega_b$ is the band width, $\omega_b$ is the band centre frequency) is less than $1/16$ which agrees with our numerical results. Obviously, such a property can only appear when the dimension of the system is larger than (or equal to) 2.

The abnormal radius-dependent property of the third band can also be explained from the Mie resonance picture too. Actually a 'heavy-photon' band (the third band in our case), quite different from common photonic bands, looks much like the tight-binding case in electronic systems. The band is dominated by the Mie resonance (in the electronic case the band is dominated by atomic orbits) and the hopping between the resonators (the cylinders) causes the resonance frequency to expand, then a band is generated. The hopping between the resonators is determined by the 'overlap integral' of the local states at two neighbouring resonators. If the overlap integral is small, then the band width is very small. This corresponds to the case when the radius of cylinders is small. But when the radius of cylinders increases, the overlap integral between the neighbouring cylinders becomes larger, so that the band width becomes larger. Based on the Mie resonance, we have calculated the overlap integrals by the tight-binding model, and shown the results in figure 6(d). We can see that the results agree with the band-width trend shown in figure 6(c).

## 5. Conclusion

In this paper, we investigate the relation between the Mie resonance and the photonic band-gap structures of 2D PCs. The important effects induced by Mie resonance on the band-gap structures are observed and three conclusions from our study are derived. First, with the radius changing but with constant index, we find that the midgap frequency and gap width increase almost linearly with increasing radius when the radius is small, then the midgap frequency crosses the Mie resonance frequency and the increase of the midgap frequency becomes saturated. The radius value where the midgap frequencies crosses the corresponding Mie resonance frequencies becomes smaller with the increase in the refractive contrast. For very large radius, all the Mie resonance frequencies fall at the corresponding bands. Based on the scattering picture and the hopping picture of Mie resonance, we can explain all these correlations between the Mie resonance and the band-gap structures. Second, it is found that the

gap-width increases rapidly when the Mie resonance frequency falls inside the corresponding gap (with the increase of the index, the Mie resonant frequency crosses the whole gap range from the upper edge to the lower edge). And when Mie resonant frequency is near the lower edge of a gap, the gap width reaches its maximum value. After that the gap width decreases very steeply with increasing index. This property clearly shows that the photonic gap width is related with scattering strength of the Mie resonance too. The field distribution of the in-gap states from the FDTD calculation also confirm the scattering effect of Mie resonance. Third, we find that for the 'heavy-photon' band (the third band in our model) the band width increases with increasing radius, which is quite different from other common bands (such as the first and second bands). From the field distribution of such bands, we can see that the hopping picture dominates the wave propagation. From the overlapping integral, which is the parameter of the hopping ability, we can explain the change in band width of 'heavy-photon' bands. From these results, we can understand more clearly how the Mie resonance influences the formation of the photonic band-gap structure. The effects of the Mie resonance on photonic band-gap structure presented in this paper could help us to find proper materials and structures for designing various kinds of PCs.

## Acknowledgments

This work has been supported by NNSFC (grant no. 10374096), SFMSBRP (grant no. 2001CCA02800), and the CAS-BaiRen programme.

## Appendix. The selection of the second gap

In this paper we define the first gap as the common case which is the frequency range between the first and second bands. But for the definition of the 'second gap', we need to be more careful.

First we discuss the case of the nearly-free-photon approximation, where the band-gap structure is from the small periodic modulation of the dielectric constant. The first three Brillouin zones (BZ) of the square lattice and band-gap structure are presented in figures A.1(a) and (b), respectively. In figure A.1(a), the shade represented by diagonal lines around the central $\Gamma$ point is the first BZ, the blank area around the first BZ is the second BZ and the shaded area of verticals around the second BZ is the third one. It is know that the third and fourth bands are folded from the third BZ, so the $k_y$ direction wavevector of the mode at these bands is equal to $G_y$ [12]. And we know that the third and fourth bands are degenerate at $\Gamma$ due to symmetry. In this paper, since we only discuss the effects of Mie resonance on the photonic band gap structure in the $k_x$ direction (suppose $k_y = 0$), we have to neglect the third and fourth bands in the weak scattering case. So that we define the 'second gap' as the frequency range between the second and *fifth* band, as shown in figure A.1(b) with index $n = 1.2$.

But when the index or the radius of cylinders increases, the third band goes down. Finally it will be degenerate with the second band at $\Gamma$ point (as shown in figure A.1(c)). Now, from the tight binding model [6] we know that the Mie resonances of the cylinder in PCs play a similar role to the atomic orbits in the electronic case. The first Mie resonance state has an axis symmetry and is corresponding to the first band. And the second Mie resonance state with a $\cos\theta$ symmetry is two-fold degenerate and will split the second and third bands due to the neighbour overlapping integral. The degeneration of the second and third bands at $\Gamma$ is due to symmetry. So, after the degeneration of the second and third bands at the $\Gamma$ point, in order to

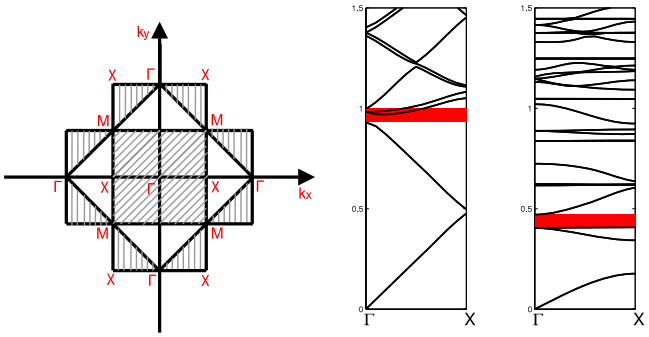


(a) Brillouin zones (b) n=1.2 (c) n=5.0

**Figure A.1.** (a) The first three Brillouin zones. The first one is shaded with diagonal lines, the blank is the second one and the vertically shaded area is the third one. (b) The band structure in the ΓX direction with very small refractive index contrast, $n = 1.2$. (c) The band structure in the ΓX direction with high refractive index contrast, $n = 5$.

discuss the effects of Mie resonance, 'the second gap' is defined as the frequency range between the third band and the fourth band, as shown in figure A.1(c).

## References


[1] Bohren C F and Huffman D R 1983 *Absorption and Scattering of Light by Small Particles* (New York: Wiley)

[2] http://www.physics.utoronto.ca/∼john/

[3] Zhang Z and Satpathy S 1990 Electromagnetic wave propagation in periodic structure: Bloch wave solution of Maxwell's equations *Phys. Rev. Lett.* **65** 2650

[4] Ohtaka K and Tanabe Y 1995 Photonic band using vector spherical waves. I. Various properties of Bloch electric fields and heavy photons *J. Phys. Soc. Japan* **65** 2265

[5] Antonoyiannakis M I and Pendry J B 1997 Mie resonances and bonding in photonic crystals *Europhys. Lett.* **40** 613

[6] Lidorikis E, Sigalas M M, Economou E N and Soukoulis C M 1998 Tight-binding parametrization for photonic band gap materials *Phys. Rev. Lett.* **81** 1405

[7] Kurokawa Y, Jimba Y and Miyazaki H 2004 Internal electric-field intensity distribution of a monolayer of periodically arrayed dielectric spheres *Phys. Rev.* B **70** 155107

[8] Vandenbem C and Vigneron J P 2005 Mie resonances of dielectric spheres in face-centred cubic photonic crystals *J. Opt. Soc. Am.* A **22** 6

[9] John S 1993 The localization of light *Photonic Band Gaps and Localization* ed C M Soukoulis (New York: Plenum) p 1

[10] Datta S, Chan C T, Ho K M, Soukoulis C M and Economou E N 1993 Photonic band gaps in periodic dielectric structures: relation to the single-scatterer Mie resonances *Photonic Band Gaps and Localization* ed C M Soukoulis (New York: Plenum) p 289

[11] Moroz A and Tip A 1997 Resonance-induced effects in photonic crystals *J. Phys.: Condens. Matter* **11** 2503

[12] Sakoda K 2001 *Optical Properties of Photonic Crystals* (Berlin: Springer) p 9

[13] Joannopoulos J D, Meade R D and Winn J N 1995 *Photonic Crystals* (Princeton, NJ: Princeton University Press) p 57

[14] Joannopoulos J D, Meade R D and Winn J N 1995 *Photonic Crystals* (Princeton, NJ: Princeton University Press) p 43

[15] Kafesaki M and Economou E N 1995 Interpretation of the band structure results for elastic and acoustic waves by analogy with the LCAO approach *Phys. Rev.* B **52** 13317